Inflammopharmacology (2022) 30:2261–2272
https://doi.org/10.1007/s10787-022-01060-5

Inflammopharmacology

ORIGINAL ARTICLE

Anti-arthritic effects of *Schisandra chinensis* extract in monosodium iodoacetate-induced osteoarthritis rats

You-Suk Lee[1,2] · Sung-Min Kim[3] · Eun-Jung Park[1,2] · Hae-Jeung Lee[1,2,4]

Received: 27 May 2022 / Accepted: 14 August 2022 / Published online: 5 September 2022

Abstract

The present study aimed to investigate the therapeutic effects of *Schisandra chinensis* (SC) extract on clinical symptoms of osteoarthritis and the modulating effect on the mechanisms associated with the progression of osteoarthritis in a rat model of monosodium iodoacetate (MIA)-induced osteoarthritis. Osteoarthritis-induced rats were randomized into four groups: MIA injection control (MC), MIA injection with celecoxib (PC), MIA injection with SC extract 100 mg/kg (SC100), and MIA injection with SC extract 200 mg/kg (SC200). Another healthy group received a saline injection as a negative control (NC). During the treatment, weight-bearing measurements were performed once a week for 4 weeks. Histopathological and biochemical analyses of the joints, blood, and chondrocyte tissue were performed following the completion of treatment. Compared with MC rats, SC rats demonstrated significantly alleviated pain behavior, bone erosion, and cartilage degradation. SC reduced serum levels of matrix metalloproteinases and pro-inflammatory cytokines. SC treatment also reversed the levels of biomarkers such as Collagen II and ADAMTS4 in the cartilage tissue. Moreover, SC administration inhibited the phosphorylation levels of nuclear factor kappa B (NF-κB) and NF-κB Inhibitor alpha. This study demonstrates that SC ameliorated osteoarthritis at in vivo level. Our results suggest that SC might be a potential therapeutic agent for osteoarthritis.

Keywords Osteoarthritis · Schisandra chinensis · Inflammatory response · NF-κB

Introduction

Osteoarthritis is the major degenerative joint disease caused by the destruction of articular cartilage and inflammation of joint tissue (Alsalem et al. 2019; Steels et al. 2019). The associated risk factors include aging, obesity, and physical joint injury (Chen et al. 2017). Inflammation of the synovial membrane, thickening of the subchondral bone, osteophyte formation, and ligament degradation are the pathological features of osteoarthritis (Chen et al. 2017; Loeser et al. 2012). With the progression of osteoarthritis, pain and swelling deteriorate, thereby ultimately reducing the quality of life (Van der Veken et al. 2017).

Inflammation is the most important cause of structural changes in chondrocytes, and elevated levels of inflammatory mediators such as tumor necrosis factor-alpha (TNFα), interleukin (IL)-1beta, IL-6, and nitric oxide (NO) have been reported in the serum and synovium chondrocytes during the progression of osteoarthritis (Fernandes et al. 2002; Gong et al. 2012; Musumeci et al. 2012). Cartilage degradation influences the production of multiple inflammatory factors such as prostaglandin E2 (PGE2), inducible nitric oxide synthase (iNOS), and cyclooxygenase-2 (COX2) (Robinson et al. 2016; Richards et al. 2016). Matrix metalloproteinases (MMPs), which are induced by inflammatory mediators participate in the matrix turnover as the major substrate proteinase (Monfort et al. 2008). The overproduction of

✉ Eun-Jung Park
ejpark@gachon.ac.kr

✉ Hae-Jeung Lee
skysea@gachon.ac.kr; skysea1010@gmail.com

1 Department of Food and Nutrition, College of BioNano Technology, Gachon University, 1342 Seongnamdaero, Sujeong-gu, Seongnam-si, Gyeonggi-do 13120, Republic of Korea

2 Institute for Aging and Clinical Nutrition Research, Gachon University, Seongnam-si, Gyeonggi-do 13120, Republic of Korea

3 Department of Food Science and Biotechnology, College of BioNano Technology, Gachon University, Seongnam-si, Gyeonggi-do 13120, Republic of Korea

4 Department of Health Sciences and Technology, GAIHST, Gachon University, Incheon, Gyeonggi-do 21999, Republic of Korea

MMPs, PGE2, and COX2 results in cartilage collapse along with proteoglycan and collagen destruction (Sellam and Berenbaum 2010; Thalhamer et al. 2008; Rahmati et al. 2016).

The aggrecanases are proteases that belong to a disintegrin and metalloproteinase with thrombospondin motifs (ADAMTS) family and play important roles in the progression of various diseases, including arthritis (Lin and Liu 2010). ADAMTS4 and ADAMTS5, which are major aggrecanases, are thought to be the critical mediators of cartilage degeneration during the development of osteoarthritis (Verma and Dalal 2011; Meng et al. 2020).

Schisandra chinensis (SC) belongs to the family *Schisandraceae* and grows in Asian countries such as Korea, China, Japan, and the far-east of Russia (Panossian and Wikman 2008; Chun et al. 2014). SC has been used in traditional medicine for the treatment of various ailments. The fruit part of SC exerts a wide range of pharmacological effects, including antioxidant (Kang et al. 2014a), anti-tumor (Lv et al. 2015), anti-inflammatory (Bae et al. 2012; Kang et al. 2014b), anti-vascular fibrotic (Jeong et al. 2015; Park et al. 2012), anti-atrophic (Kim et al. 2015), and anti-diabetic effects (Kwon et al. 2011).

To the best of our knowledge, there exists only a little research on the effects of SC on inflammatory response and cartilage degradation in monosodium iodoacetate (MIA)-induced osteoarthritis rats, even though several studies have reported the antioxidant and anti-inflammatory effects of the SC. This study aimed to investigate whether SC extract exhibits anti-arthritic and modulating effects on the mechanisms associated with the development of osteoarthritis in a rat model.

Materials and methods

Materials

The SC extract was provided by BIOPORTKOREA Inc. (Busan, Korea). SC extract was prepared using the standard production processes by the company. Briefly, dried fruit of SC was extracted in 20% ethyl alcohol for 4 h at 90 °C. After filtration, the extract was concentrated under reduced pressure. Freeze-drying was carried out to obtain the final product in powder form. The SC extract contained approximately 4.92 ± 0.06 mg/g of schizandrin as a specific ingredient by high-performance liquid chromatography analysis (Kim et al. 2018). The SC extract was protected from light and stored at 4 °C to protect it from degradation until use.

Animals and treatments

Male Sprague–Dawley (SD) rats were supplied by Orient Bio. Ltd. (Gyeonggi-do, Korea) and acclimated for 1 week under standard conditions (temperature; 20–25 °C, humidity; 50–55%, and a 12 h light–dark cycle) with free access to food and water ad libitum. After 7 days of acclimation, the animals were randomly divided into five groups ($n = 7$ for each group): (1) NC, normal control (saline injection); (2) MC, MIA injection control; (3) PC, MIA injection with celecoxib 3 mg/kg as a positive control (TCI, Tokyo, Japan); (4) SC100, MIA injection with SC 100 mg/kg; and (5) SC200, MIA injection with SC 200 mg/kg. The MIA solution (2 mg/50ul of 0.9% saline) was injected directly into the intra-articular space of the right knee while the rats were under anesthesia with a 2% isoflurane O_2 mixture. Rats in the NC and MIA groups were orally given 0.9% saline. The experimental extracts dissolved in 0.9% saline were orally administered every day for 4 weeks. Once a week, the body weight was measured. All animals were cared for and used in accordance with the guidelines of Gachon University for the care and use of laboratory animals (approval number: GIACUC-R2021014). After 12 h of fasting, all mice were anesthetized with CO_2. Blood samples were collected by cardiac puncture and clotted in the serum-separating tube before centrifugation at $2000 \times g$ for 20 min at 4 °C. Serum was aliquoted and stored at − 80 °C until use. Articular cartilages were immediately dissected from rats and stored at − 80 °C until analysis. The experimental design is shown in Fig. 1. To establish a dose–response relationship, three different doses were initially chosen in our preliminary study: (1) SC100, MIA injection with SC 100 mg/kg; (2) SC200, MIA injection with SC 200 mg/kg; and (3) SC400, MIA injection with SC 400 mg/kg (data not shown); and two concentrations (SC100 and SC200) were chosen based on clinical trial applicability.

Weight-bearing measurement

After MIA injection, weight-bearing capacity measurement of the hind limbs of the rats was performed with the Incapacitance Meter Tester 600 (IITC Life Science, Woodland Hills, CA, USA) as a pain measurement (Jo et al. 2020). Weight-bearing ratios were recorded once a week. The weight distribution ratio was calculated using the following equation:

$$\left[\text{weight in right hind limb} / (\text{weight in right hind limb} + \text{weight in left hind limb})\right] \times 100.$$

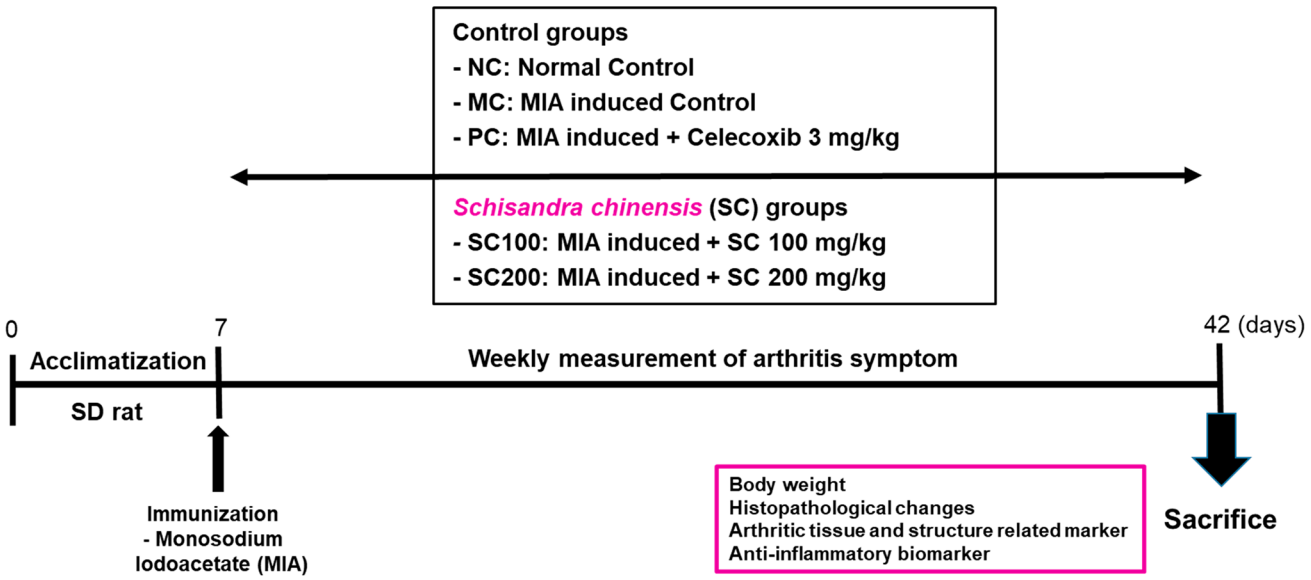

Fig. 1 Experimental design of the study

Biochemical assays

The serum levels of C-reactive protein (CRP), nitric oxide (NO), cartilage oligomeric matrix protein (COMP), hyaluronic acid (HA), MMPs, aggrecan (ACAN), IL-6, TNF-α, IL-1β, and PGE2 were measured using an enzyme-linked immunosorbent assay (ELISA) kit (R&D system, Minneapolis, MN, USA) according to the manufacturer's protocols.

Micro-computed tomography (Micro-CT)

The isolated knee joint was scanned using a Skyscan Micro-CT (Bruker, Billerica, MA, USA). After fixing the specimen on a jig for Micro-CT measurement using parafilm, images were acquired with a tube voltage of 90 kV and a current of 88 uA. The obtained cross-section images were aligned for each cross-section, and the morphometric parameters were measured using Skyscan CT-analyzer software (Bruker, Billerica, MA, USA).

The bone mineral density (BMD, mm), percent bone volume (PBV, %), porosity (%), bone volume/tissue volume (BV/TV, mm^3), bone surface/tissue volume (BS/TV, mm^2/mm^3), trabecular thickness (Tb.Th, mm), trabecular number (Tb.N, 1/mm), and trabecular separation (Tb.Sp, mm) of the metaphysis of the tibia were analyzed to evaluate the structural changes.

Histological and immunohistochemical (IHC) assay

Knee joints of the rat were fixed with 10% formalin solution (Sigma–Aldrich, St. Louis, MO, USA), decalcified using 10% ethylene diamine tetraacetic acid (EDTA), embedded in paraffin, and serially sectioned. Tissue sections were stained with hematoxylin and eosin (H&E, DAKO, Glostrup, Denmark) and Safranin O (Sigma–Aldrich, MO, USA). Paraffin sections were blocked with 1% bovine serum albumin and incubated for 1 h at 37 °C with a collagen 2 antibody (Abcam, Cambridge, UK). The image scan was photographed using a digital slide scanner (PANNORAMIC 250 Flash III, 3DHISTECH Ltd. Budapest, Hungary) and observed using a Caseviewer (3DHISTECH Ltd. Budapest, Hungary). Histological changes were evaluated using the Osteoarthritis Research Society International (OARSI) guidelines. Image-Pro® 10 program (Media Cybernetics, Inc, Rockville, MD, USA) was used to assess the level of collagen II expression in the entire area.

Real-time PCR analysis

Total RNA was extracted from the articular cartilages using an RNA extraction kit (iNtRON Biotechnology, Gyeonggi-do, Korea). cDNA was synthesized from RNA (50 ng/μL) using a GoScript™ Reverse Transcriptase (Promega, Madison, WI, USA) and used for real-time RT-PCR with a SYBR Premix Ex Taq II (Takara, Otsu, Japan) using an ABI QuantStudio 3 (Applied Biosystems, Foster City, CA, USA). Primer sequences used for RT-PCR are displayed in Table 1.

Western blot analysis

Articular cartilages were homogenized in a PRO-PREP™ Protein Extraction Solution (iNtRON Biotechnology,

Table 1 Primer sequence used for quantitative real-time RT-PCR

Genes	Primer sequence (5′–3′)	Accession number
iNOS	Forward: CAC CAC CCT CCT TGT TCA AC	NM_012611.3
	Reverse: CAA TCC ACA ACT CGC TCC AA	
COX2	Forward: CCA GCA GGC TCA TAC TGA TAG GA	NM_017232.3
	Reverse: GCA GGT CTG GGT CGA ACT TG	
Collagen II	Forward: GAG TGG AAG AGC GGA GAC TA	NM_012929.1
	Reverse: GTC TCC ATG TTG CAG AAG AC	
ADAMTS4	Forward: GCC AGC AAC CGA GGT CCC AT	NM_023959.1
	Reverse: TTG GCA GCG GCG GCC ATG AC	
ADAMTS5	Forward: CCG CAC CTC GAA ACA GTG GC	NM_198761.2
	Reverse: CAC CTG CGT ATT TGG GAA CC	
GAPDH	Forward: TGG TGA AGG TCG GTG TGA AC Reverse: TTC CCA TTC TCA GCC TTG AC	NM_017008

Real-time RT-PCR real-time reverse transcription-polymerase chain reaction; i*NOS* inducible nitric oxide synthase; *COX2* cyclooxygenase-2; *Collagen II* type II collagen; *ADAMTS4* ADAM metallopeptidase with thrombospondin type 1 Motif 4; *ADAMTS5* ADAM metallopeptidase with thrombospondin type 1 Motif 5; *GAPDH* glyceraldehyde 3-phosphate dehydrogenase

Gyeonggi-do, Korea) containing the Halt™ phosphatase inhibitor cocktail (Thermo Scientific, Waltham, MA, USA). After quantification with the BCA assay (Thermo Scientific, Waltham, MA, USA), protein samples (20 μg) were separated by 10% SDS polyacrylamide gel electrophoresis and subsequently transferred to a polyvinylidene difluoride (PVDF) membrane (Merck Millipore, Bedford, MA, USA). The membranes were blocked with 5% skim milk for 1 h at room temperature, and then washed and incubated with the primary antibodies at 4 °C overnight. Antibodies against nuclear factor kappa B (NF-κB) p65, phospho-NF-κB p65 (Ser536), phospho-NF-κB Inhibitor alpha (IκBα) (Ser32), and GAPDH were purchased from Cell Signaling Technology (Danvers, MA, USA). Horseradish peroxidase (HRP)-conjugated secondary antibodies were purchased from Promega (Madison, WI, USA). The WEST-Queen™ RTS Western Blot Detection Kit (iNtRON Biotechnology, Gyeonggi-do, Korea) was used to detect the signals, and the immunoreactive bands were visualized by chemiluminescence using the ImageQuant LAS 500 imager (GE Healthcare Life Sciences, Little Chalfont, UK).

Statistical analyses

All data are presented as mean ± standard deviation (SD). Statistical differences were determined with a one-way analysis of variance (ANOVA) followed by Duncan's multiple range test. Two-group comparisons were carried out with Student's *t* test using SPSS 25 (SPSS Inc., Chicago, IL, USA). Values of $P < 0.05$ were considered statistically significant.

Table 2 Bodyweight and weight gain of each group

Groups	NC	MC	PC	SC100	SC200
Bodyweight after randomization (g) [A]	206.48 ± 10.54 ^{ns}	206.21 ± 12.13	206.16 ± 9.45	206.07 ± 6.09	206.19 ± 4.95
Terminal body weight (g) [B]	427.68 ± 42.64 ^{ns}	421.60 ± 62.18	398.40 ± 22.19	402.06 ± 36.82	400.56 ± 37.77
Bodyweight gain (g) [B-A]	221.20 ± 33.31 ^{ns}	215.39 ± 52.28	192.24 ± 28.28	195.99 ± 31.02	194.37 ± 34.13

The data are presented as mean ± SD ($n = 7$). Statistical differences were determined by one-way ANOVA, with Duncan's multiple range tests ($p < 0.05$)

NC normal control; *MC* MIA injection control; *PC* MIA injection with celecoxib 3 mg/kg; *SC100* MIA injection with SC 100 mg/kg; *SC200* MIA injection with SC 200 mg/kg; *ns* non-significant

Table 3 Weight-bearing ratio

Groups	NC	MC	PC	SC100	SC200
Before MIA injection	50.43 ± 2.48 ns	50.65 ± 2.95	50.90 ± 4.95	50.44 ± 3.37	50.87 ± 4.18
After MIA injection					
1-week	49.81 ± 4.56^{b}	26.41 ± 4.16^{a}	30.80 ± 6.19^{a}	29.77 ± 3.71^{a}	30.24 ± 3.21^{a}
2-weeks	49.58 ± 4.03^{c}	27.14 ± 4.26^{a}	31.19 ± 3.52^{b}	30.04 ± 5.16^{b}	30.45 ± 6.62^{b}
3-weeks	49.04 ± 3.38^{c}	27.55 ± 5.61^{a}	35.02 ± 4.45^{b}	32.49 ± 5.47^{b}	33.99 ± 5.63^{b}
4-weeks	49.45 ± 6.46^{d}	28.44 ± 3.76^{a}	42.14 ± 3.06^{c}	35.38 ± 3.24^{b}	36.93 ± 3.55^{b}

The data are presented as mean ± SD ($n = 7$). Different letters indicate significant differences by one-way ANOVA, with Duncan's multiple range tests ($p < 0.05$)

NC normal control; *MC* MIA injection control; *PC* MIA injection with celecoxib 3 mg/kg; *SC100* MIA injection with SC 100 mg/kg; *SC200* MIA injection with SC 200 mg/kg; *ns* non-significant

Results

Effects of SC extract on body weight and weight-bearing distribution

As shown in Table 2, there was no significant difference among groups in terms of initial body weight, terminal body weight, and body weight gain. Weight-bearing distribution was reduced in all the groups after MIA injection. No significant differences were observed in the weight-bearing distribution among the MIA injected groups in the first week. However, the weight-bearing ratio of the PC, SC100, and SC200 groups were gradually increased and significantly higher than those of the MC group from the second week (Table 3).

Effects of SC extract on bone architecture and cartilage damage

To evaluate the anti-osteoarthritis effect of SC, micro-CT scans with three-dimensional remodeling were performed on MIA-induced osteoarthritis rats. 3- and 2-dimensional micro-CT scans of the MC group revealed erosion of the subchondral and irregular articular surfaces. After SC administration, the formation of subchondral erosion and the irregular articular surface was reduced (Fig. 2 A–C). The BMD of the MC group was lower than that of the SC groups; however, there was no significant difference in the BMD. As for the PBV (Percent Bone Volume), the PBV of the SC groups was higher than that of the MC group. The porosity result showed the lowest ratio in the NC group and the highest in the MC group; whereas it was lower in the SC groups than that in the MC group. The BV/TV (bone volume/tissue volume) and the BS/TV (bone surface/tissue volume) analysis showed a significant difference in the values between the NC group and the MIA group; whereas the values were higher in the SC groups than the MC group. The Tb.Th (trabecular thickness) and the Tb.N (trabecular number) of the MC group were lower than those of the SC groups. Tb.Sp (trabecular separation) showed the highest value in the MC group, but there was no significant difference in the values among all the groups (Table 4).

Effects of SC extract on histological characteristics

The knee joints were evaluated histologically to investigate the degree of inflammation and cartilage damage using H&E, Safranin O, and immunochemical staining. The H&E staining results demonstrated that the synovial tissue and cartilage were normally located in the NC group, and there were more synovial tissue loss and cartilage deformation in the MC group than in the NC group (Fig. 3A). Synovial tissue loss and cartilage deformation were relatively decreased in the PC group and the SC groups compared to the MC group. Safranin O staining revealed that the cartilage of the NC group was rich in proteoglycan, the destruction or erosion of the articular cartilage was severe, and the loss of proteoglycan was large in the MC group (Fig. 3B). The OARSI score in the PC, SC100, and SC200 groups was significantly lower than in the MC group (Fig. 3D). IHC staining results demonstrated that the brown-stained collagen II was abundantly distributed in the experimental groups compared with the MC group (Fig. 3C, E).

Effects of SC extract on serum biochemical parameters

Serum biochemical parameter levels were measured after isolating serum from blood collected from each experimental group. First, the effects of SC extract on serum inflammatory parameters were investigated. As can be seen in Fig. 4A–C, the MC group showed higher serum CRP, NO, and PGE2 levels than the PC, SC100, and SC200 groups. We also investigated the effects of SC on serum joint parameters. The ACAN level was significantly higher in the SC200 group compared with that of the MC group. The COMP level in the PC, SC100, and SC200 groups was significantly reduced compared with that of the MC group. The HA level in the

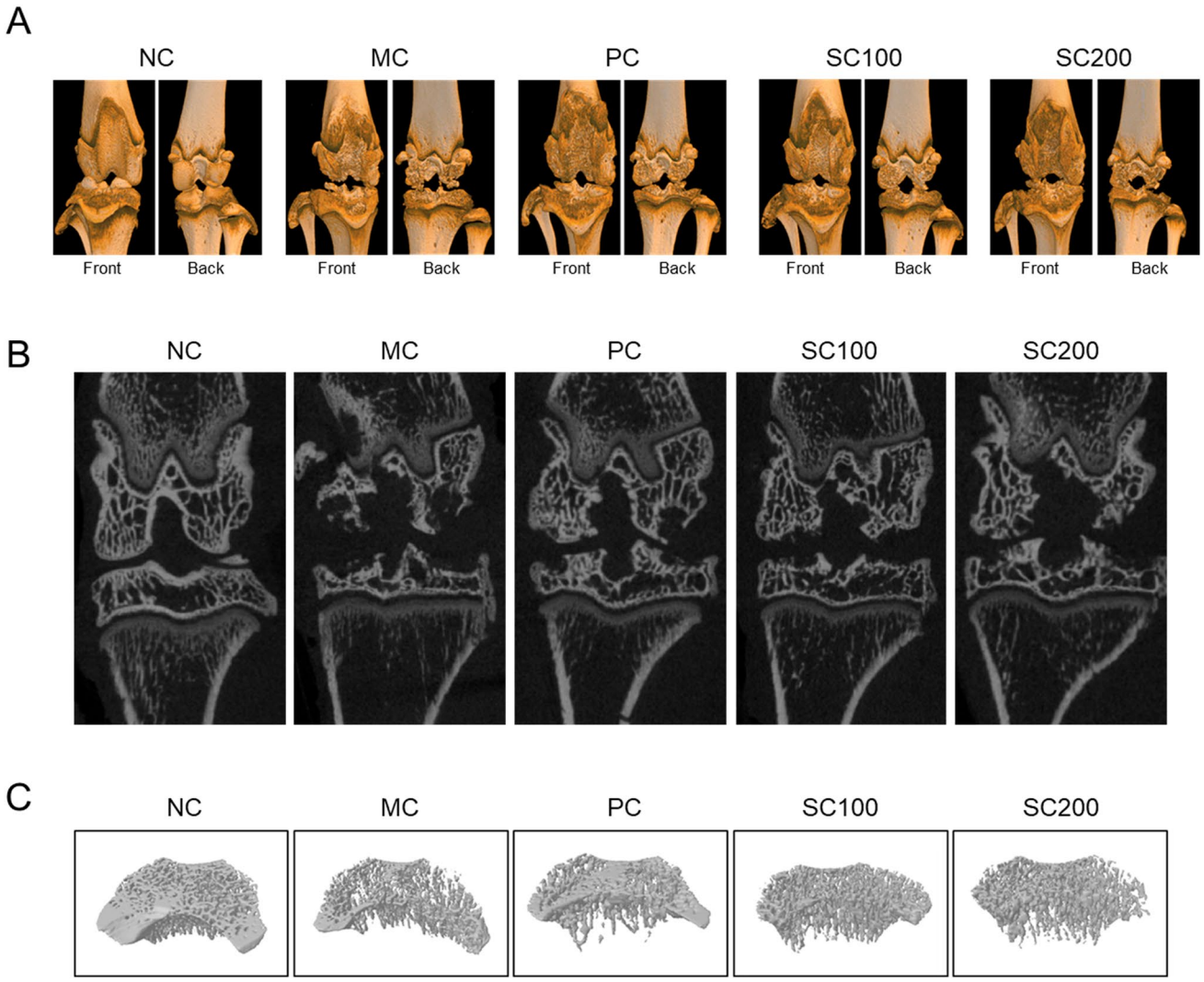

Fig. 2 Effects of SC extract on representative micro-computed tomography images. **A** Three-dimensional micro-CT images. **B** Two-dimensional micro-CT images. **C** Grayscale reconstructed images. *NC* normal control; *MC* MIA injection control; *PC* MIA injection with celecoxib 3 mg/kg; *SC100* MIA injection with SC 100 mg/kg; *SC200* MIA injection with SC 200 mg/kg

Table 4 Structural parameters by micro-CT analysis of the tibia

Groups	NC	MC	PC	SC100	SC200
BMD (mm)	0.21 ± 0.02^{b}	0.16 ± 0.01^{a}	0.16 ± 0.01^{a}	0.17 ± 0.01^{ab}	0.18 ± 0.01^{ab}
PBV (%)	26.81 ± 7.51^{b}	8.36 ± 3.72^{a}	9.96 ± 2.71^{a}	14.19 ± 3.08^{a}	16.17 ± 2.64^{ab}
Porosity (%)	73.19 ± 7.51^{a}	91.64 ± 3.72^{b}	90.04 ± 2.71^{b}	85.81 ± 3.08^{b}	83.83 ± 2.64^{ab}
BV/TV (mm^3)	0.27 ± 0.08^{b}	0.08 ± 0.04^{a}	0.10 ± 0.03^{a}	0.11 ± 0.05^{a}	0.12 ± 0.03^{a}
BS/TV (mm^2/mm^3)	7.69 ± 1.25^{b}	3.30 ± 1.04^{a}	4.09 ± 0.89^{a}	5.34 ± 0.83^{ab}	5.80 ± 1.19^{ab}
Tb.Th (mm)	0.13 ± 0.01^{b}	0.10 ± 0.01^{a}	0.10 ± 0.01^{a}	0.11 ± 0.01^{a}	0.11 ± 0.01^{ab}
Tb.N (1/mm)	2.02 ± 0.38^{b}	0.79 ± 0.28^{a}	1.00 ± 0.22^{a}	1.32 ± 0.24^{ab}	1.43 ± 0.35^{ab}
Tb.Sp (mm)	0.43 ± 0.05^{ns}	0.58 ± 0.20	0.48 ± 0.07	0.50 ± 0.03	0.47 ± 0.01

The data are presented as mean ± SD (n = 7). Different letters indicate significant differences by one-way ANOVA, with Duncan's multiple range tests ($p < 0.05$)

BMD bone mineral density; *PBV* percent bone volume; *BV/TV* bone volume/tissue volume; *BS/TV* bone surface/tissue volume; *Tb.Th* trabecular thickness; *Tb.N* trabecular number; *Tb.Sp* trabecular separation. *NC* normal control; *MC* MIA injection control; *PC* MIA injection with celecoxib 3 mg/kg; *SC100* MIA injection with SC 100 mg/kg; *SC200* MIA injection with SC 200 mg/kg

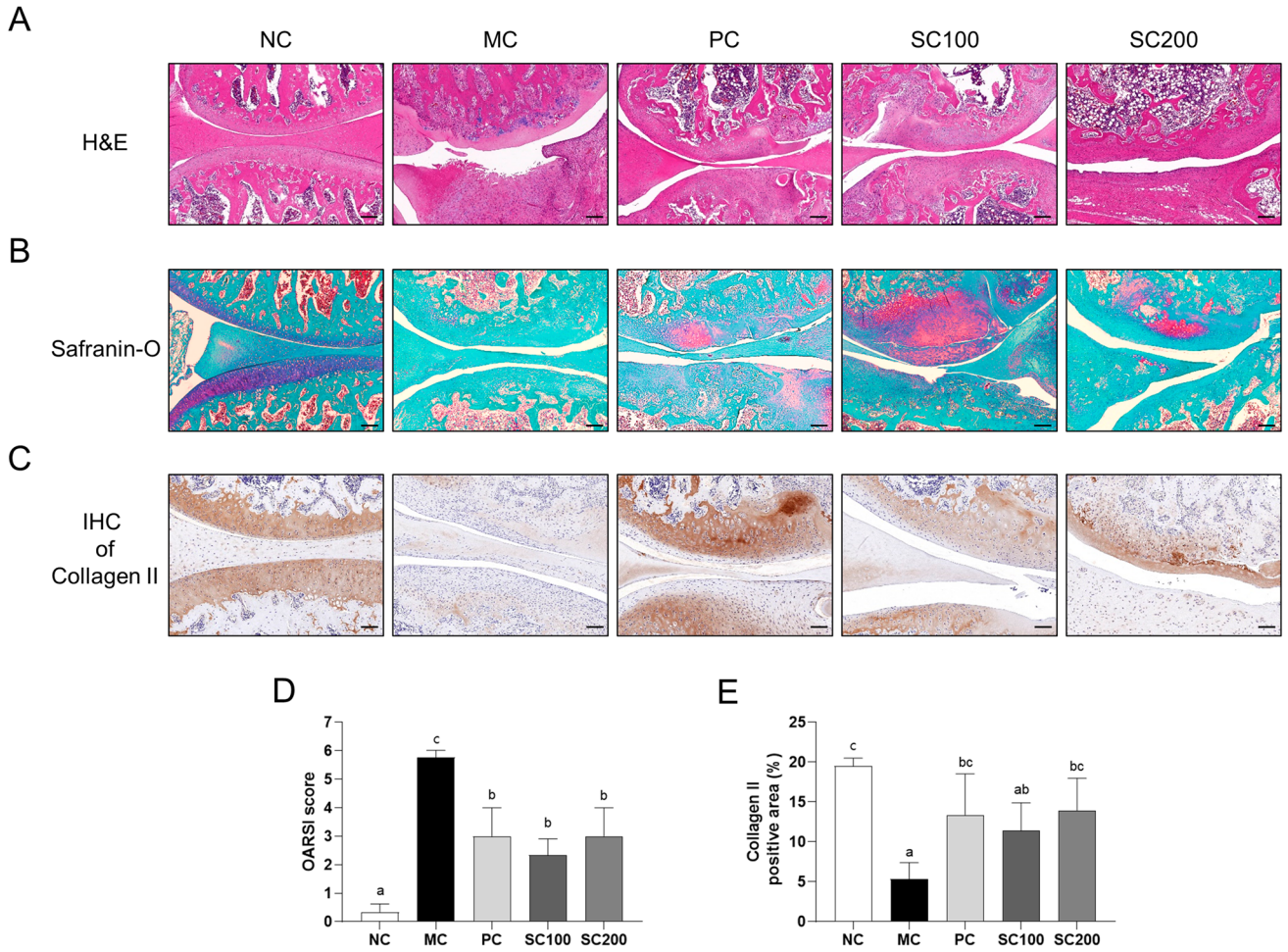

Fig. 3 Effects of SC extract on histopathological changes. **A** H&E staining results. **B** Safranin O staining results. **C** Immunohistochemistry results. The scale bar indicates 200 μm. **D** OARSI scores as examined by histopathological changes. **E** Average area for Collagen II Immunohistochemical assay. *NC* normal control; *MC* MIA injection control; *PC* MIA injection with celecoxib 3 mg/kg; *SC100* MIA injection with SC 100 mg/kg; *SC200* MIA injection with SC 200 mg/kg. Different letters indicate significant differences by one-way ANOVA, with Duncan's multiple range tests ($p < 0.05$)

NC, PC, SC100, and SC200 groups showed significantly lower values compared to the MC group (Fig. 4D–F). To determine the effects of SC on MMPs, the serum levels of MMP-2, MMP-9, and MMP-13 were measured. As can be seen in Fig 4G–I, the MMP level in the MC group was significantly higher than that of the SC groups. In addition, the SC administrated groups showed significantly lower IL-1β, IL-6, and TNF-α levels than the MC group. There was no significant difference in the levels of inflammatory cytokines between the SC groups (Fig. 4J–L).

Effects of SC extract on the expression of osteoarthritis-related mRNA markers

We also investigated the effects of SC extract on the mRNA expression of iNOS, COX2, ADAMTS4, ADAMTS5, and collagen II in the cartilages. As shown in Fig. 5A, B, the mRNA expression of iNOS and COX2 in SC groups was significant reduced compared to the MC group. The mRNA expression of Collagen II in the MC group was also lower than that of the SC groups (Fig. 5C). The ADAMTS4 mRNA expression in the MC group was significantly higher than that of the SC200 group. The ADAMTS5 mRNA expression in the MC group was higher compared to the SC groups; however, there was no significant difference in the ADAMTS5 mRNA expression among the groups (Fig. 5D, E).

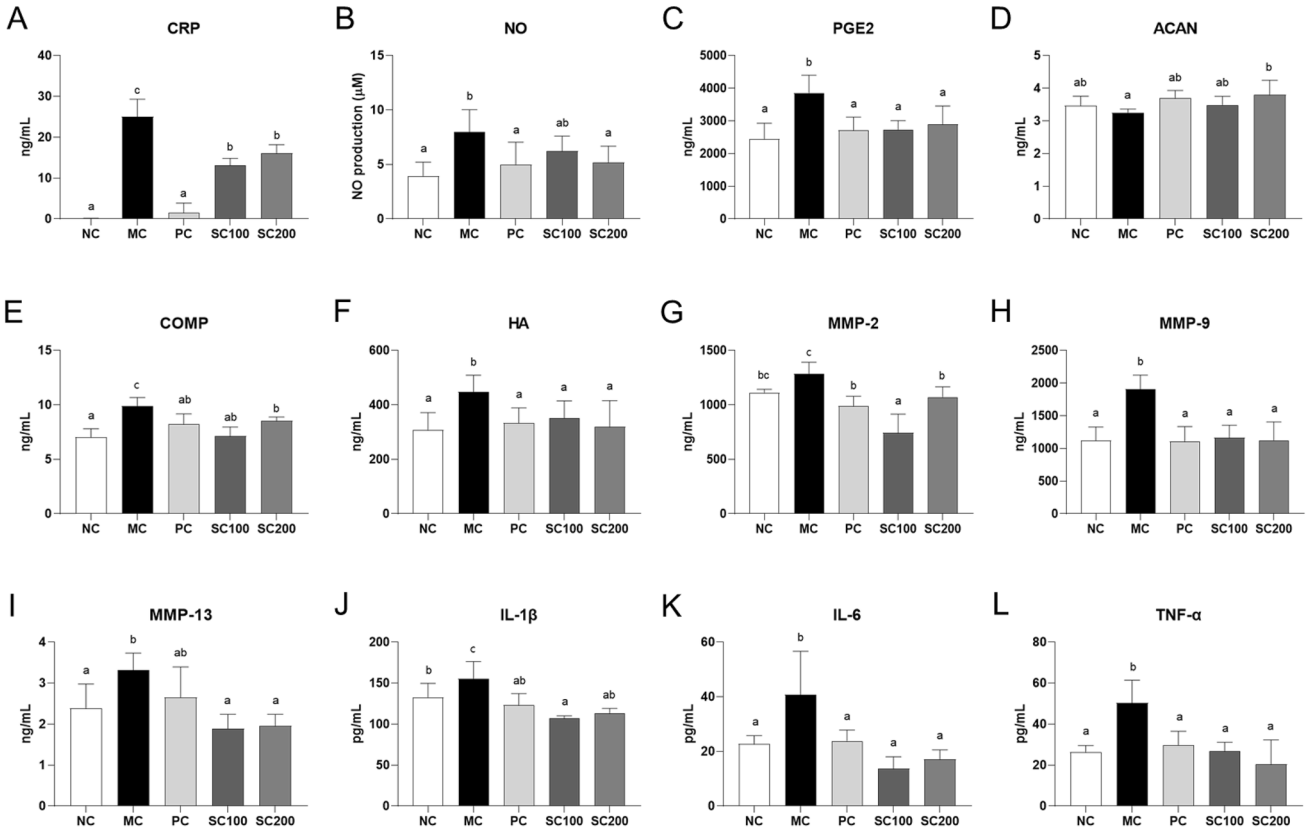

Fig. 4 Effects of SC extract on serum biochemical parameters. **A** CRP, C-reactive protein. **B** NO, nitric oxide. **C** PGE2, prostaglandin E2. **D** ACAN, aggrecan. **E** COMP, cartilage oligomeric matrix protein. **F** HA, hyaluronic acid. **G** MMP-2, matrix metalloproteinases-2. **H** MMP-9, matrix metalloproteinases-9. **I** MMP-13, matrix metalloproteinases-13. **J** IL-1β, interleukin-1β. **K** IL-6, interleukin-6. **L** TNF-α, tumor necrosis factor-α. *NC* normal control; *MC* MIA injection control; *PC* MIA injection with celecoxib 3 mg/kg; SC100, MIA injection with SC 100 mg/kg; *SC200* MIA injection with SC 200 mg/kg. The data are presented as mean ± SD ($n = 7$). Different letters indicate significant differences by one-way ANOVA, with Duncan's multiple range tests ($p < 0.05$)

Effects of SC extract on NF-κB activation

To understand the mechanisms of action of SC in the osteoarthritis model, we examined the phosphorylation status of NF-κB and IκBα by Western blot. As can be seen in Fig. 6A, B the MC group demonstrated significantly elevated levels of phosphorylation of NF-κB and IκBα in the cartilages, whereas the SC groups had lower levels of phospho-NF-κB and phospho-IκBα.

Discussion

Currently, available osteoarthritis medications are used to treat pain and inflammation (CHEA Tantowi 2018). Although these chemical drugs have demonstrated efficacy, long-term uses of these drugs have serious side effects such as cardiovascular problems, renal dysfunctions, diarrhea, and gastrointestinal disorders (Sharma et al. 2020; CROFFORD 2013; Graverand-Gastineau 2010). Thus, the development of osteoarthritis therapeutics that are effective, safe, and have minimal adverse effects is of immense importance (Lee et al. 2019).

Numerous studies over the decades have reported that herbal extracts relieve chondrocyte inflammation, thereby controlling pain with improvement in joint function (Jhun et al. 2018; Wang et al. 2018). Recent research indicates that *Schisandra chinensis* (SC) exhibits anti-inflammatory properties and may be beneficial for osteoarthritis (Jeong et al. 2017). In the present study, it was confirmed that SC extract increased the weight-bearing ratio and prevented synovial inflammation, cartilage destruction, and bone-margin erosion in MIA-induced osteoarthritis rats.

Several inflammatory factors affect cartilage degradation, including NO, PGE2, iNOS, and COX2 (Robinson et al. 2016; Richards et al. 2016). Elevated levels of pro-inflammatory cytokines such as IL-1β, IL-6, and TNF-α have been found in serum and chondrocytes with the progression

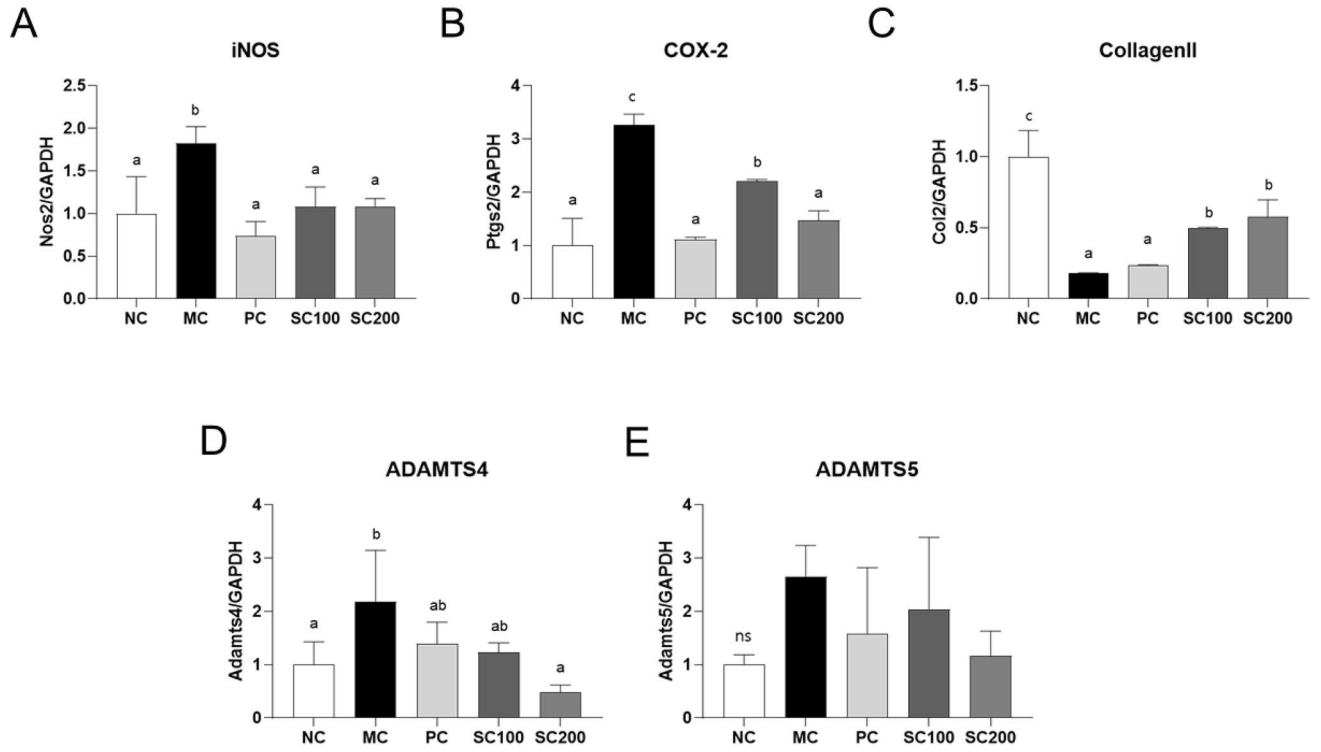

Fig. 5 Effects of SC extract on the mRNA expression. **A** iNOS, inducible NO synthase. **B** COX2, cyclooxygenase-2. **C** Collagen II, collagen type II. **D** ADAMTS4, ADAM metallopeptidase with thrombospondin type 1 Motif 4. **E** ADAMTS5, ADAM metallopeptidase with thrombospondin type 1 Motif 5. *NC* normal control; *MC* MIA injection control; PC, MIA injection with celecoxib 3 mg/kg; *SC100* MIA injection with SC 100 mg/kg; *SC200* MIA injection with SC 200 mg/kg. The data are presented as mean ± SD ($n = 7$). Different letters indicate significant differences by one-way ANOVA, with Duncan's multiple range tests ($p < 0.05$)

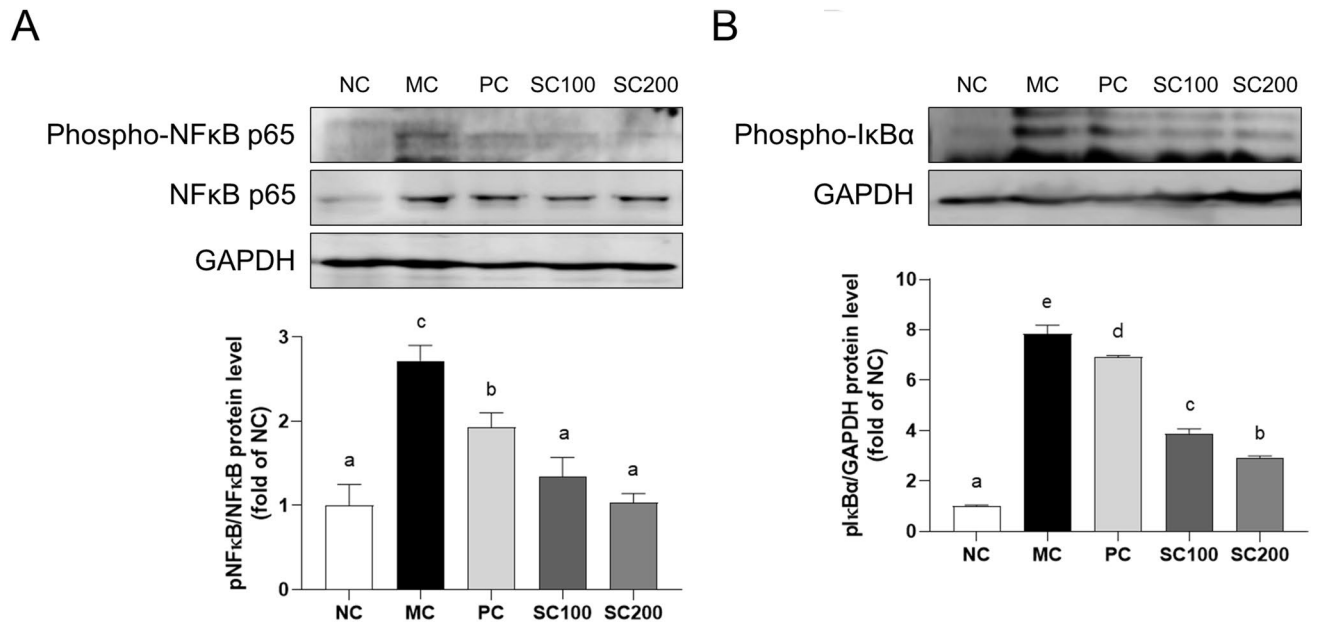

Fig. 6 Effects of SC extract on the protein expression and protein phosphorylation levels. **A** NF-κB, nuclear factor-κB. **B** IκBα, NF-κB Inhibitor alpha. *NC* normal control; *MC* MIA injection control; *PC* MIA injection with celecoxib 3 mg/kg; *SC100* MIA injection with SC 100 mg/kg; *SC200* MIA injection with SC 200 mg/kg. The data are presented as mean ± SD ($n = 3$). Different letters indicate significant differences by one-way ANOVA, with Duncan's multiple range tests ($p < 0.05$)

of osteoarthritis (Fernandes et al. 2002; Gong et al. 2012; Musumeci et al. 2012). In this study, SC extract led to reduce in pro-inflammatory cytokines and inflammatory-related mediators. Furthermore, RNA expression of iNOS and COX2 in articular tissue was significantly higher in the MC group than in the SC treatment groups. Matrix metalloproteinases (MMPs) are the major substrate proteinases that participate in matrix turnover and are induced by inflammatory mediators (Monfort et al. 2008). In this study, decreased levels of MMP-2, MMP-9, and MMP-13 were observed in the SC groups. These findings suggest that SC protects knee joints from inflammatory responses and joint degradation, which leads to the progression and development of osteoarthritis.

The proteases known as ADAMTS play a crucial role in various disease processes such as inflammation and arthritis. (Lin and Liu 2010). Evidence has been established that ADAMTS and MMPs are related to each other and can cleave aggrecan (Meng et al. 2020). In this study, the MC group demonstrated the highest levels of mRNA expression of ADAMTS4 and ADAMTS5, as well as the highest levels of MMPs. It is thought that aggrecan concentration was decreased in the MC group because of the increased ADAMTS4, ADAMTS5, and MMPs levels. On the other hand, the SC group showed reduced levels of ADAMTS and MMPs. These observations suggest that SC can ameliorate the cleavage of aggrecan through down-regulation of the ADAMTS.

NF-κB is a transcription factor that plays an important role in the regulation of inflammatory responses (Mulero et al. 2019). NF-κB activation is triggered by signal-induced degradation of IκB protein (Liang et al. 2020). Phosphorylation of NF-κB and IκB leads to the transcription of target genes such as iNOS, COX2, and MMPs (Chen et al. 2014). In the present study, the phosphorylation status of NF-κB and IκBα was investigated. Our findings demonstrated that SC extract significantly decreased the phosphorylation of NF-κB and IκBα, thereby suggesting that SC modulates the inflammatory response caused by cartilage damage, thus restoring the damage to the cartilage. The main contributing ingredient of SC extract is Schizandrin, a representative lignan of *Schisandra chinensis*. The anti-inflammatory effects of Schizandrin have been steadily reported in various cell types, including macrophages (Moon et al. 2012; Guo et al. 2009; Park et al. 2011), supporting our findings of anti-arthritic effects of SC extract.

Conclusions

SC extract significantly alleviated MIA-induced pain behavior and inflammation in rat model of osteoarthritis. SC extract also reversed the levels of biomarkers such as Collagen II and ADAMTS4 in the cartilage tissue. Moreover, SC extract administration inhibited the phosphorylation of NF-κB and IκBα. Our findings suggest that SC extract could potentially improve osteoarthritis susceptibility.

Acknowledgements We express thanks to the research assistants for their efforts in the successful execution of this study at the Department of Food and Nutrition, Gachon University, Republic of Korea.

Author contributions Y-SL, E-JP, and H-JL conceived the study. Y-SL and S-MK conducted all the experiment. Y-SL and E-JP analyzed and visualized the data, and they also wrote the original draft. H-JL revised the manuscript. H-JL and E-JP provided supervision. H-JL is responsible for project administration. All authors read and approved the final manuscript.

Funding This work was supported by the "Food Functionality Evaluation program" under the Ministry of Agriculture, Food and Rural Affairs and partly by the Korea Food Research Institute.

Data availability The data used to support the findings of this study are available from the corresponding authors upon request.

Declarations

Conflict of interest The author(s) declare no potential competing interest.

Ethics approval Animal experiments were carried out according to the national regulations of the usage and welfare of laboratory animals and approved by the Gachon University for Institutional Animal Care and Use Committee (approval number: GIACUC-R2021014).

References

Alsalem M, Haddad M, Aldossary SA, Kalbouneh H, Altarifi A, Jaffal SM, Abbas MA, Aldaoud N, El-Salem K (2019) Role of cannabinoid receptor 1 and the peroxisome proliferator-activated receptor alpha in mediating anti-nociceptive effects of synthetic cannabinoids and a cannabinoid-like compound. Inflammopharmacology 27:1131–1142

Bae H, Kim R, Kim Y, Lee E, KIM HJ, Jung YPJSK, Kim J (2012) Effects of *Schisandra chinensis* Baillon (Schizandraceae) on lipopolysaccharide induced lung inflammation in mice. J Ethnopharmacol 142:41–47

Chen YJ, Tsai KS, Chan DC, Lan KC, Chen CF, Yang RS, Liu SH (2014) Honokiol, a low molecular weight natural product, prevents inflammatory response and cartilage matrix degradation in human osteoarthritis chondrocytes. J Orthop Res 32:573–580

Chen D, Shen J, Zhao W, Wang T, Han L, Hamilton JL, Im HJ (2017) Osteoarthritis: toward a comprehensive understanding of pathological mechanism. Bone Res 5:16044

Chun JN, Cho M, So I, Jeon JH (2014) The protective effects of *Schisandra chinensis* fruit extract and its lignans against cardiovascular disease: a review of the molecular mechanisms. Fitoterapia 97:224–233

Crofford LJ (2013) Use of NSAIDs in treating patients with arthritis. Arthritis Res Ther 15(Suppl 3):S2

Fernandes JC, Martel-Pelletier J, Pelletier JP (2002) The role of cytokines in osteoarthritis pathophysiology. Biorheology 39:237–246

Gong D, Geng C, Jiang L, Wang L, Yoshimura H, Zhong L (2012) Mechanisms of olive leaf extract-ameliorated rat arthritis caused by kaolin and carrageenan. Phytother Res 26:397–402

Graverand-Gastineau LEMP (2010) Disease modifying osteoarthritis drugs: facing development challenges and choosing molecular targets. Curr Drug Targets 11:528–535

Guo LY, Hung TM, Bae K, Jang S, Shin EM, Chung JW, Kang SS, Kim HP, Kim YS (2009) Effects of schisandrin on transcriptional factors in lipopolysaccharide-pretreated macrophages. Arch Pharm Res 32:399–405

Jeong JW, Kim JW, Ku SK, Kim SG, Kim KY, Kim GY, Hwang HJ, Kim BW, Chung HY, Kim CM, Choi YH (2015) Essential oils purified from Schisandrae semen inhibits tumor necrosis factor-alpha-induced matrix metalloproteinase-9 activation and migration of human aortic smooth muscle cells. BMC Complement Altern Med 15:7

Jeong JW, Kim J, Choi EO, Kwon DH, Kong GM, Choi IW, Kim BH, Kim GY, Lee KW, Kim KY, Kim SG, Choi YW, Hong SH, Park C, Choi YH (2017) *Schisandrae fructus* ethanol extract ameliorates inflammatory responses and articular cartilage damage in monosodium iodoacetate-induced osteoarthritis in rats. EXCLI J 16:265–277

Jhun JY, Na HS, Shin JW, Jung KA, Seo HB, Ryu JY, Choi JW, Moon SJ, Park HJ, Oh SW, Cho ML, Min JK (2018) Notoginseng Radix and Rehmanniae Radix Preparata extract combination (YH23537) reduces pain and cartilage degeneration in rats with monosodium iodoacetate-induced Osteoarthritis. J Med Food 21:745–754

Jo HG, Lee GY, Baek CY, Song HS, Lee D (2020) Analgesic and anti-inflammatory effects of aucklandia lappa root extracts on acetic acid-induced writhing in mice and monosodium iodoacetate-induced osteoarthritis in rats. Plants 10:42

Kang JS, Han MH, Kim GY, Kim CM, Kim BW, Hwang HJ, Hyun Y (2014a) Nrf2-mediated HO-1 induction contributes to antioxidant capacity of a *Schisandrae fructus* ethanol extract in C2C12 myoblasts. Nutrients 6:5667–5678

Kang YS, Han MH, Hong SH, Park C, Hwang HJ, Kim BW, Kyoung KH, Choi YW, Kim CM, Choi YH (2014b) Anti-inflammatory effects of Schisandra chinensis (Turcz.) baill fruit through the inactivation of nuclear factor-kappaB and mitogen-activated protein kinases signaling pathways in lipopolysaccharide-stimulated murine macrophages. J Cancer Prev 19:279–287

Kim JW, Ku SK, Kim KY, Kim SG, Han MH, Kim GY, Hwang HJ, Kim BW, Kim CM, Choi YH (2015) *Schisandrae fructus* supplementation Ameliorates Sciatic neurectomy-induced muscle atrophy in mice. Oxid Med Cell Longev 2015:872428

Kim KY, Ku SK, Lee KW, Song CH, An WG (2018) Muscle-protective effects of *Schisandrae fructus* extracts in old mice after chronic forced exercise. J Ethnopharmacol 212:175–187

Kwon DY, Kim DS, Yang HJ, Park S (2011) The lignan-rich fractions of Fructus Schisandrae improve insulin sensitivity via the PPAR-gamma pathways in in vitro and in vivo studies. J Ethnopharmacol 135:455–462

Lee YM, Son E, Kim SH, Kim DS (2019) Effect of Alpinia oxyphylla extract in vitro and in a monosodium iodoacetate-induced osteoarthritis rat model. Phytomedicine 65:153095

Liang WJ, Yang HW, Liu HN, Qian W, Chen XL (2020) HMGB1 upregulates NF-kB by inhibiting IKB-alpha and associates with diabetic retinopathy. Life Sci 241:117146

Lin EA, Liu CJ (2010) The role of ADAMTSs in arthritis. Protein Cell 1:33–47

Loeser RF, Goldring SR, Scanzello CR, Goldring MB (2012) Osteoarthritis: a disease of the joint as an organ. Arthritis Rheum 64:1697–1707

Lv XJ, Zhao LJ, Hao YQ, Su ZZ, Li JY, Du YW, Zhang J (2015) Schisandrin B inhibits the proliferation of human lung adenocarcinoma A549 cells by inducing cycle arrest and apoptosis. Int J Clin Exp Med 8:6926–6936

Meng P, Zhang F, Zhang Y, Wei H, Tan S, Guo X, Wang S, Yu Y (2020) ADAMTS4 and ADAMTS5 may be considered as new molecular therapeutic targets for cartilage damages with Kashin-Beck disease. Med Hypotheses 135:109440

Monfort J, Tardif G, Roughley P, Reboul P, Boileau C, Bishop PN, Pelletier JP, Martel-Pelletier J (2008) Identification of opticin, a member of the small leucine-rich repeat proteoglycan family, in human articular tissues: a novel target for MMP-13 in osteoarthritis. Osteoarthritis Cartilage 16:749–755

Moon PD, Jeong HJ, Kim HM (2012) Effects of schizandrin on the expression of thymic stromal lymphopoietin in human mast cell line HMC-1. Life Sci 91:384–388

Mulero MC, Huxford T, Ghosh G (2019) NF-kappaB, IkappaB, and IKK: integral components of immune system signaling. Adv Exp Med Biol 1172:207–226

Musumeci G, Carnazza ML, Leonardi R, Loreto C (2012) Expression of beta-defensin-4 in "an in vivo and ex vivo model" of human osteoarthritic knee meniscus. Knee Surg Sports Traumatol Arthrosc 20:216–222

Panossian A, Wikman G (2008) Pharmacology of *Schisandra chinensis* Bail.: an overview of Russian research and uses in medicine. J Ethnopharmacol 118:183–212

Park SY, Park DJ, Kim YH, Kim Y, Kim SG, Shon KJ, Choi YW, Lee SJ (2011) Upregulation of heme oxygenase-1 via PI3K/Akt and Nrf-2 signaling pathways mediates the anti-inflammatory activity of Schisandrin in *Porphyromonas gingivalis* LPS-stimulated macrophages. Immunol Lett 139:93–101

Park EJ, Chun JN, Kim SH, Kim CY, Lee HJ, Kim HK, Park JK, Lee SW, So I, Jeon JH (2012) Schisandrin B suppresses TGFbeta1 signaling by inhibiting Smad2/3 and MAPK pathways. Biochem Pharmacol 83:378–384

Rahmati M, Mobasheri A, Mozafari M (2016) Inflammatory mediators in osteoarthritis: a critical review of the state-of-the-art, current prospects, and future challenges. Bone 85:81–90

Richards MM, Maxwell JS, Weng L, Angelos MG, Golzarian J (2016) Intra-articular treatment of knee osteoarthritis: from anti-inflammatories to products of regenerative medicine. Phys Sportsmed 44:101–108

Robinson WH, Lepus CM, Wang Q, Raghu H, Mao R, Lindstrom TM, Sokolove J (2016) Low-grade inflammation as a key mediator of the pathogenesis of osteoarthritis. Nat Rev Rheumatol 12:580–592

Sellam J, Berenbaum F (2010) The role of synovitis in pathophysiology and clinical symptoms of osteoarthritis. Nat Rev Rheumatol 6:625–635

Sharma VK, Mamontov E, Tyagi M (2020) Effects of NSAIDs on the nanoscopic dynamics of lipid membrane. Biochim Biophys Acta Biomembr 1862:183100

Steels E, Venkatesh R, Steels E, Vitetta G, Vitetta L (2019) A double-blind randomized placebo controlled study assessing safety, tolerability and efficacy of palmitoylethanolamide for symptoms of knee osteoarthritis. Inflammopharmacology 27:475–485

Tantowi CHEA, Lau NASF, Mohamed S (2018) Ficus deltoidea prevented bone loss in preclinical Osteoporosis/Osteoarthritis Model by suppressing inflammation. Calcif Tissue Int 103:388–399

Thalhamer T, McGrath MA, Harnett MM (2008) MAPKs and their relevance to arthritis and inflammation. Rheumatology 47:409–414

van der Veken D, Curvers F, Fieuws S, Lambrechts P (2017) Prevalence of apical periodontitis and root filled teeth in a Belgian subpopulation found on CBCT images. Int Endod J 50:317–329

Verma P, Dalal K (2011) ADAMTS-4 and ADAMTS-5: key enzymes in osteoarthritis. J Cell Biochem 112:3507–3514

Wang F, Shi L, Zhang Y, Wang K, Pei F, Zhu H, Shi Z, Tao T, Li Z, Zeng P, Wang X, Ji Q, Qin L, Xue Q (2018) A traditional herbal formula xianlinggubao for pain control and function improvement in patients with knee and hand osteoarthritis: a multicenter, randomized, open-label, controlled trial. Evid Based Complement Alternat Med 2018:1827528